Journal of Medicinal Chemistry

Article

pubs.acs.org/jmc

# A Cereblon Modulator (CC-220) with Improved Degradation of Ikaros and Aiolos

Mary E. Matyskiela, Weihong Zhang, Hon-Wah Man, George Muller, Godrej Khambatta, Frans Baculi, Matthew Hickman, Laurie LeBrun, Barbra Pagarigan, Gilles Carmel, Chin-Chun Lu, Gang Lu, Mariko Riley, Yoshitaka Satoh, Peter Schafer, Thomas O. Daniel, James Carmichael, Brian E. Cathers, and Philip P. Chamberlain*

[1]Celgene Corporation, 10300 Campus Point Drive, Suite 100, San Diego, California 92121, United States

Supporting Information

**ABSTRACT:** The drugs lenalidomide and pomalidomide bind to the protein cereblon, directing the CRL4−CRBN E3 ligase toward the transcription factors Ikaros and Aiolos to cause their ubiquitination and degradation. Here we describe CC-220 (compound **6**), a cereblon modulator in clinical development for systemic lupus erythematosis and relapsed/refractory multiple myeloma. Compound **6** binds cereblon with a higher affinity than lenalidomide or pomalidomide. Consistent with this, the cellular degradation of Ikaros and Aiolos is more potent and the extent of substrate depletion is greater. The crystal structure of cereblon in complex with DDB1 and compound **6** reveals that the increase in potency correlates with increased contacts between compound **6** and cereblon away from the modeled binding site for Ikaros/Aiolos. These results describe a new cereblon modulator which achieves greater substrate degradation via tighter binding to the cereblon E3 ligase and provides an example of the effect of E3 ligase binding affinity with relevance to other drug discovery efforts in targeted protein degradation.

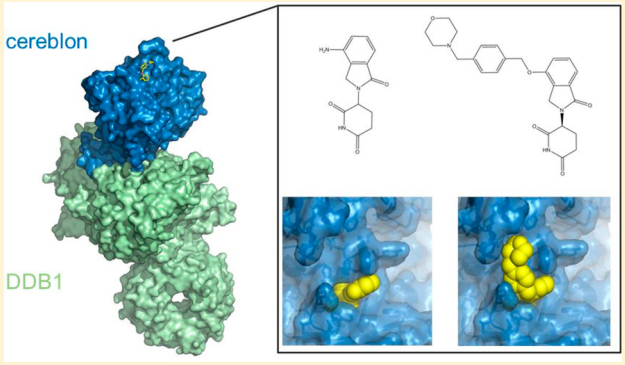


## INTRODUCTION

Lenalidomide and pomalidomide are immunomodulatory drugs that are clinically effective in the treatment of cancer, including newly diagnosed and relapsed multiple myeloma.[1] These drugs target cereblon (CRBN), a substrate receptor for the CRL4 (CUL4−RBX1−DDB1) ubiquitin ligase complex.[2] Rather than inhibiting cereblon, ligand binding confers neomorphic activity, altering the substrate specificity of the ubiquitin ligase by promoting the recruitment of substrate proteins. Bound substrates are ubiquitinated by the cereblon−CRL4 complex, leading to their degradation by the 26S proteasome, thereby driving the clinical activity in myeloma.[3] Ikaros and Aiolos (encoded by the genes IKZF1 and IKZF3, respectively) were the first cereblon substrates to be identified, and it was demonstrated that the addition of cereblon modulating ligands triggers their recruitment and degradation.[4] Ikaros and Aiolos are zinc finger transcription factors with critical roles in hematological development and differentiation,[5] and the downstream effects of degrading these proteins mediate the antiproliferative and immunomodulatory activities of lenalidomide and pomalidomide.[6] Polymorphisms in both IKZF1 and IKZF3 are associated with a risk of developing systemic lupus erythematosus (SLE).[7]

Lenalidomide is further approved for use in 5q-deletion-associated myelodysplastic syndrome, where clinical activity has been associated with degradation of an additional substrate, the protein kinase Ck1a.[16] In addition, the translation termination factor GSPT1 has now been described as a ligand-directed substrate of the cereblon,[8] highlighting the potential breadth of activity of cereblon modulators, as now three unrelated classes of substrate proteins, zinc finger transcription factors, protein kinases, and protein translation factors, have been targeted. The work on CK1a and GSPT1 further demonstrates the potential for ligand-substrate specificity, as CK1a is targeted to cereblon by lenalidomide but not by pomalidomide, and GSPT1 is targeted by a recently reported cereblon modulator[8b] but not by either lenalidomide or pomalidomide. Cereblon modulators therefore provide an important proof-of-principle for the further development of compounds targeting specific proteins for destruction that may have previously been considered undruggable.

Structural studies have shown that cereblon modulators bind to cereblon through the glutarimide moiety, which docks into a hydrophobic tritryptophan pocket formed by Trp380, Trp386,

**Special Issue:** Inducing Protein Degradation as a Therapeutic Strategy

**Received:** January 13, 2017




DOI: 10.1021/acs.jmedchem.6b01921
J. Med. Chem. XXXX, XXX, XXX−XXX

and Trp400.[9] This binding mode leaves the insoindolinone/phthalimide ring of the compounds exposed on the cereblon surface, and it was predicted that this would form a hotspot of unsatisfied hydrogen bonds that would mediate substrate binding via direct protein−protein interactions.[8a,9a] Subsequent structural and mutagenesis studies on cereblon−substrate complexes have confirmed this hypothesis and surprisingly revealed that unrelated proteins CK1a and GSPT1 bind to cereblon through a common structural feature, thereby defining a degron.[8b,10] The enhancement of protein−protein interactions by a small molecule is highly reminiscent of the "molecular glue" mechanism described for the plant hormones auxin and jasmonate.[11] This mechanism contrasts with the linker-based approaches, where heterobifunctional ligands recruit substrates to a ligase via distinct small molecule binding events on each side of a linker.[12]

Here we describe the cereblon modulator CC-220 (compound **6**),[13] which is currently in phase 2 clinical trials for the treatment of systematic lupus erythematosus (SLE) and phase 1b/2a clinical trials for relapsed and refractory multiple myeloma (MM). We demonstrate that compound **6** has a higher affinity for cereblon than lenalidomide or pomalidomide. Consistent with these findings, compound **6** has a higher potency for the cellular degradation of Ikaros and Aiolos. The crystal structure of compound **6** bound to CRBN−DDB1 reveals that there are additional contacts with the surface of cereblon compared to lenalidomide or pomalidomide. These results provide a demonstration that increased target degradation can be achieved by alterations of the ligand binding affinity for the ligase and supports the further evaluation of compound **6** in the clinic.

## RESULTS

**Compound 6 Is a Cereblon Modulator with Improved Biochemical and Cellular Potencies.** Like lenalidomide and pomalidomide, compound **6** contains a glutarimide ring that binds in the try-tryptophan pocket of cereblon and an isoindolinone ring that can interact with both cereblon and substrates (Figure 1a). In addition, the chemical structure of compound **6** is extended compared to lenalidomide and pomalidomide, containing additional phenyl and morpholino moieties enabling further interactions with cereblon or substrates. To determine the relative binding affinities between lenalidomide, pomalidomide, and compound **6**, we used a TR-FRET cereblon binding assay to determine the $IC_{50}$ values for these compounds. This assay monitors the displacement of a Cy5-conjugated cereblon modulating compound (compound **7**) from the tri-trp pocket of CRBN. Under these assay conditions, the $IC_{50}$ values for lenalidomide and pomalidomide were similar at 1.5 and 1.2 $\mu$M, respectively, while compound **6** exhibited significantly higher affinity with an $IC_{50}$ of approximately 60 nM (Figure 1b). $IC_{50}$s for lenalidomide and pomalidomide have been previously reported in multiple assay formats. The potencies reported here are comparable to the values determined from thermal shift studies, where lenalidomide and pomalidomide showed similar potencies toward cereblon (both ∼3 $\mu$M).[3a] A fluorescence polarization-based assay reported ∼10-fold more potent binding (∼150 nM),[9b] however this is likely due to the different assay formats, and lenalidomide and pomalidomide were approximately equipotent which is consistent with this study. A cereblon FRET assay has also been previously reported,[14] however the concentrations of protein used would preclude assessment of potent compounds such as compound **6**.

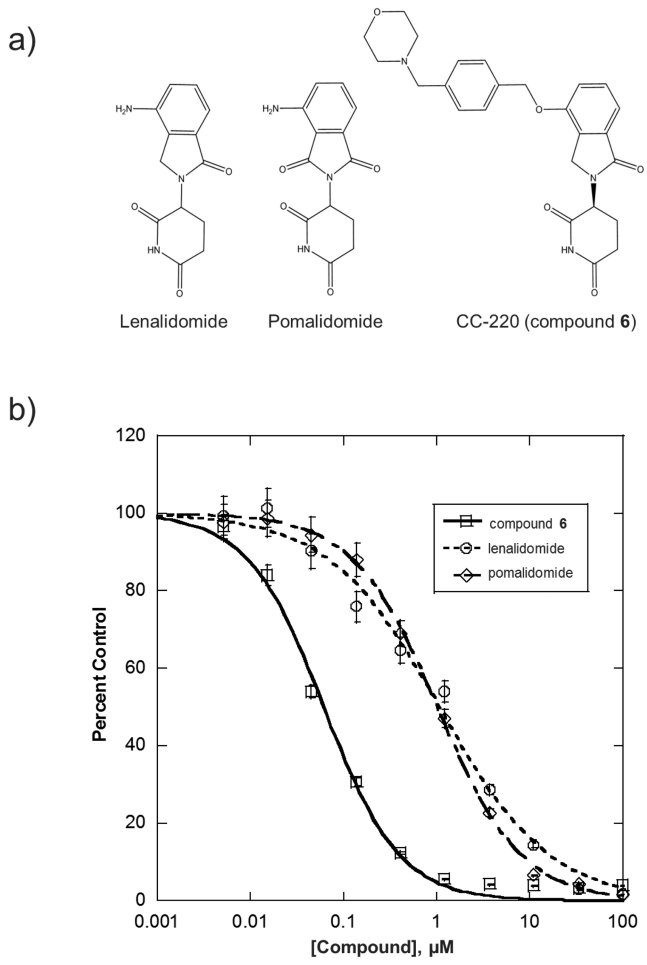


**Figure 1.** (a) Chemical structures of selected clinical stage cereblon modulators including compound **6**. (b) Determination of the relative cereblon binding affinities for compound **6**, lenalidomide, and pomalidomide by TR-FRET. $IC_{50}$s under these conditions were 1.5 $\mu$M for lenalidomide (circles), 1.2 $\mu$M for pomalidomide (diamonds), and 60 nM for compound **6** (squares).

Consistent with increased biochemical binding affinity, we also observe greater potency of compound **6** in cellular degradation assays measuring the ligand-dependent depletion of Ikaros or Aiolos. However, compound **6** does not significantly degrade GSPT1 or CK1$\alpha$ (Supporting Information, Figure S1, and data not shown). To measure the effects of compound treatment on Ikaros and Aiolos degradation in cells, we used a cell-based assay that follows the chemiluminescent signal of proteins incorporating an ePL tag. We find that treatment with compound **6** results in the loss of Ikaros protein levels with an $EC_{50}$ of 1 nM compared to 67 nM for lenalidomide and 24 nM for pomalidomide. Compound **6** is similarly potent toward Aiolos, with an $EC_{50}$ of 0.5 nM compared to 87 nM for lenalidomide and 22 nM for pomalidomide. In addition, the extent of substrate depletion is more dramatic with compound **6**, indicating more efficient substrate degradation relative to the rate of protein resynthesis. The increase in the cellular degradation potency of compound **6** corresponds with the increase in binding affinity observed in the biochemical assay, suggesting that the increase in cereblon affinity likely contributes to the increase in cellular potency. In contrast, the 3−4-fold increase in cellular potency observed for pomalidomide compared to lenalidomide is more likely driven by other


DOI: 10.1021/acs.jmedchem.6b01921
J. Med. Chem. XXXX, XXX, XXX−XXX

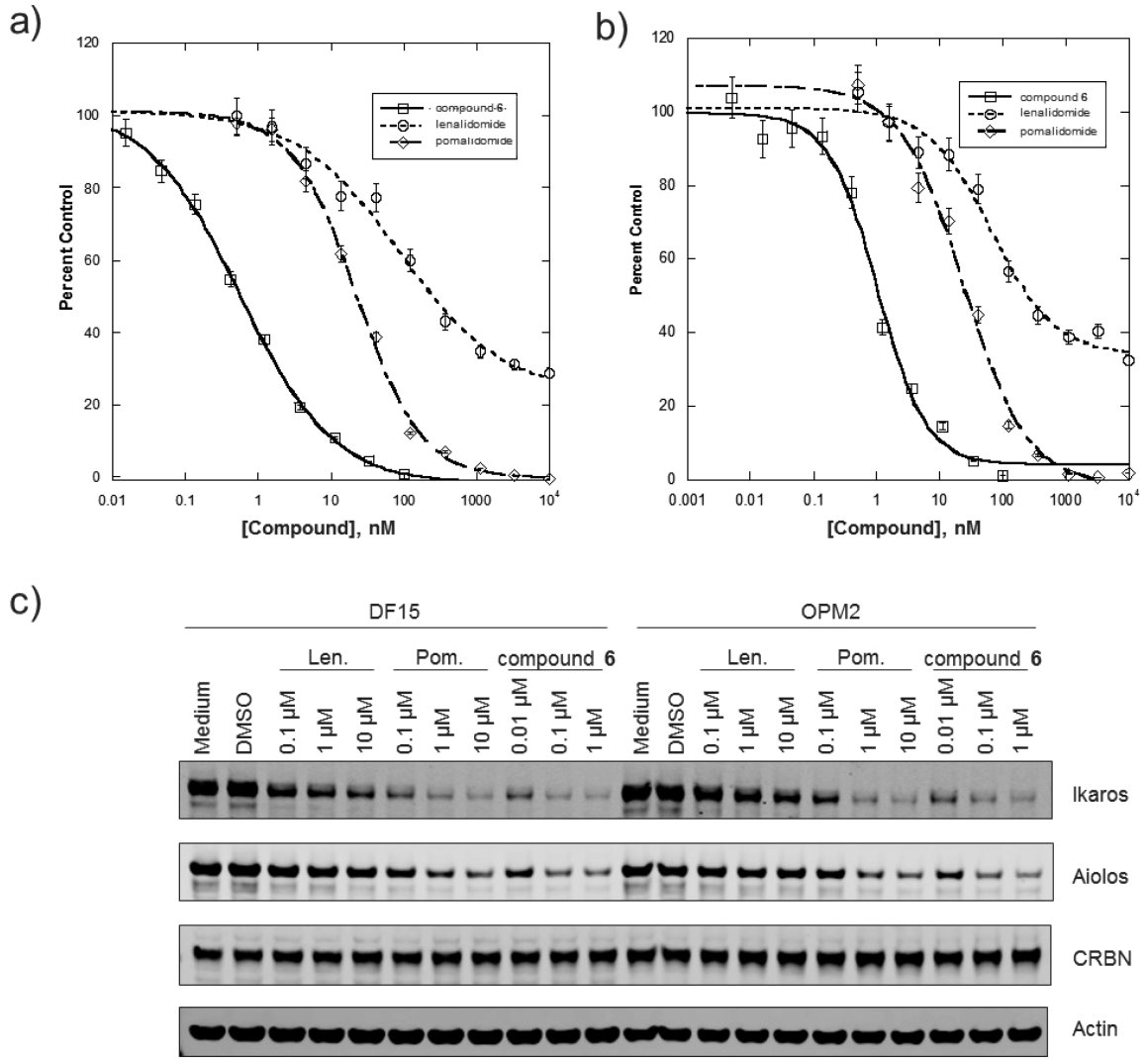


**Figure 2.** (a) Quantitation of Ikaros degradation with chemiluminescent cell-based assay. $EC_{50}$s determined were 67 nM for lenalidomide (circles), 24 nM for pomalidomide (diamonds), and 1 nM for compound **6** (squares). (b) Quantitation of Aiolos degradation with chemiluminescent cell-based assay. $EC_{50}$s determined were 87 nM for lenalidomide (circles), 22 nM for pomalidomide (diamonds), and 0.5 nM for compound **6** (squares). (c) Immunoblot analysis of whole-cell extracts of DF15 and OPM2 cells incubated for 5 h with DMSO, lenalidomide, pomalidomide, or compound **6** at the indicated concentrations.

factors, such as the alteration of substrate recruitment affinity or physicochemical properties of the compound.

To confirm these effects are relevant with respect to the endogenous proteins, we treated DF15 and OPM2 myeloma cell lines[3a,15] with lenalidomide, pomalidomide, and compound **6** for 5 h (Figure 2c). Compound **6** treatment led to greater degradation of Ikaros and Aiolos compared to lenalidomide and pomalidomide, consistent with the results from the chemiluminescence-based cellular degradation assay.

**Crystal Structure of Cereblon in Complex with DDB1 and Compound 6.** To examine the mechanism of higher affinity binding by compound **6**, we determined the crystal structure of the ternary complex of compound **6** bound to human cereblon (aa 40−442) and human DDB1 (full length) at 3.2 Å resolution. Data collection statistics are in Supporting Information, along with sample electron density (Supporting Information, Table S1 and Figure S3). The overall structure was highly similar to the previously reported cereblon−DDB1 structures, with the binding site for cereblon modulators on the opposite face of cereblon compared to the DDB1 interaction site.

The glutarimide ring of compound **6** binds in the tri-trp pocket in a similar binding mode to the previously reported structures, and the isoindolinone ring is presented on the surface in a similar binding mode to lenalidomide and other reported analogues[8b,9,10] (Figure 3, for a detailed structural comparison of compound **6** and lenalidomide binding modes, see Supporting Information, Figure S2). Compound **6** has an extended structure compared to lenalidomide and pomalidomide (Figure 1a), and the crystal structure shows that the phenyl ring of compound **6** is positioned inside a groove on the cereblon surface formed by E377, H378, P352, and H353 (Figure 3a). The morpholine ring is oriented toward a hydrophobic pocket formed of residues I154 and F102, however this moiety is poorly defined in the electron density, possibly due to motion (Supporting Information, Figure S3). F150 is positioned adjacent to the morpholino group of compound **6**, in contrast to some other structures, where this is found in an extended conformation (Figure 3b[8b,9a]). However, this conformation should be interpreted with caution as F150 occurs at the apex of a loop that has exhibited mobility in other structures, and often participates in crystal lattice contacts.



DOI: 10.1021/acs.jmedchem.6b01921
J. Med. Chem. XXXX, XXX, XXX−XXX

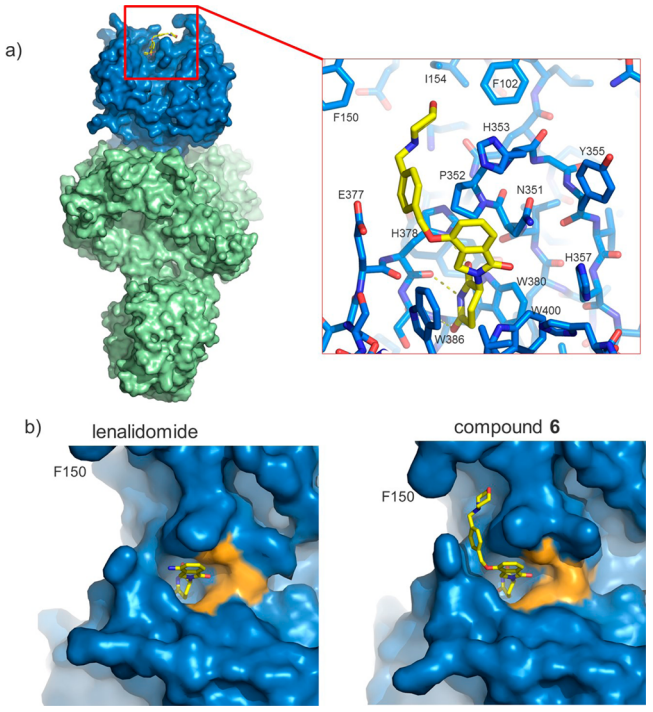


**Figure 3.** (a) The crystal structure of cereblon (blue) in complex with DDB1 (green) and compound **6** (yellow sticks). Inset: detail of bound compound **6**, with the glutarimide ring docked in the tri-trp pocket and the phenyl ring extending from the isoindolinone positioned in a groove formed by E377, H378, P352, and H353 of cereblon. (b) Comparison of the binding surface interactions of lenalidomide (yellow, PDB 4TZ4, left panel) and compound **6** (yellow, this study, right panel) with cereblon (blue, surface representation). Cereblon surface residues that were previously shown to mediate binding to Ikaros by mutational studies are shown in orange.[8b] The amino acid side chain F150 is labeled.

The structures of cereblon in complex with CK1a and GSPT1 revealed that the primary site of cereblon substrate interactions is shared between the characterized substrates, and docking and mutagenesis studies predicted the same site of interaction for Ikaros and Aiolos.[8b,10] This site of interaction is formed by three hydrogen bond donors on cereblon, N351, H357, and W400, which are positioned proximal to the isoindolinone or phthalimide rings of bound cereblon modulators (Figure 3a). These residues (shown in orange surface representation in Figure 3b) are positioned away from the phenyl and morpholine rings of compound **6**, such that differences in compound activity are unlikely to be the result of direct substrate interactions of these moieties with Ikaros or Aiolos. Instead, a comparison of the crystal structures of lenalidomide and compound **6** bound to cereblon−DDB1 reveals that the observed increase in affinity correlates well with the increased surface interactions between compound **6** and cereblon (Figure 3b).

## DISCUSSION AND CONCLUSIONS

These results describe a new cereblon modulator which achieves potent cellular degradation of the transcription factors Ikaros and Aiolos. We find that the cellular potency increase correlates with a higher affinity between compound **6** and cereblon, which is likely driving higher occupancy of cereblon in the cell and effectively increasing the active fraction of cereblon−CRL4 enzyme capable of binding to substrate. The extended chemical moieties relative to lenalidomide and pomalidomide appear to enhance the surface area of compound **6** that contacts cereblon, which correlates with the observed binding affinity increase in biochemical assays. Furthermore, the 20-fold increase in binding affinity in vitro observed compared to lenalidomide correlates well with the increased potency of compound **6** in cellular degradation of Ikaros and Aiolos. However, potency increases are not always driven by enhanced cereblon binding affinity. For example, lenalidomide and pomalidomide have similar $IC_{50}$ values in the TR-FRET assay (Figure 1) and yet pomalidomide is 3−4-fold more potent than lenalidomide in the cell-based chemiluminescent degradation assays. In this case, additional factors including increased affinity for substrates, physcicochemical properties, or other pharmacological differences may be contributing to the differences in compound potency.

The crystal structures of cereblon−DDB1 in complex with the bound substrates CK1a or GSPT1 revealed a common site of interaction on the cereblon surface, which docking and mutagenesis studies indicated are shared by Ikaros. It is interesting, therefore, to consider whether the modified structure of compound **6** would in some way contribute to the cereblon−Ikaros interaction. As shown in Figure 3b, the phenyl and morpholino groups of compound **6** are positioned in an orientation away from the site where the zinc finger domain of Ikaros is predicted to interact on the surface of cereblon, indicating that the observed differences in potency are more likely to be driven by the improved compound **6**−cereblon interactions than by additional substrate interactions. This system will benefit from a kinetic analysis of substrate and compound binding in order to fully characterize the contributions of cereblon versus substrate binding and ubiquitination to the increased potency of the compound.

Robust ligand-directed substrate degradation requires many sequential steps (ligand binding, substrate recruitment, ubiquitination, release, proteosomal degradation), representing a potentially complex system for medicinal chemistry optimization compared to classical small molecule inhibitors. As such, there are many factors that could lead to alteration of cellular efficacy of a ligase modulator. This study describes one strategy for improving substrate degradation rates by enhancing ligand interactions and affinity with the ligase while describing a next-generation clinical stage cereblon modulator with improved activity against Ikaros and Aiolos. The resulting increase in potency is expected to contribute to clinical outcomes in the treatment of both SLE and relapsed/refractory MM.

## EXPERIMENTAL SECTION

**Chemistry.** Proton and carbon magnetic resonance ($^1$H NMR and $^{13}$C NMR) spectra were recorded on a Bruker UltraShield 300 spectrometer and are reported in ppm relative to the reference solvent of the sample in which they were run. HPLC and LC-MS analyses were conducted using a Waters Aquity HPLC system and Water Aquity PDA detector at 240 nm with the MS detection using Waters Aquity SQ spectrometer. All flash column chromatography was performed on EM Science silica gel 60 (particle size of 40−60 $\mu$m). All reagents were purchased from commercial sources and used without further purification unless otherwise noted. All reactions were performed under an inert atmosphere. HPLC analyses were performed using the following conditions.

All final compounds had an HPLC purity of ≥95% unless specifically mentioned.

**HPLC Method.** A linear gradient ($t$ = 0 min, 5% B; $t$ = 15 min, 95% B) using 5% acetonitrile, 95% water with 0.1% phorsphoric acid


DOI: 10.1021/acs.jmedchem.6b01921
J. Med. Chem. XXXX, XXX, XXX−XXX

**Scheme 1**

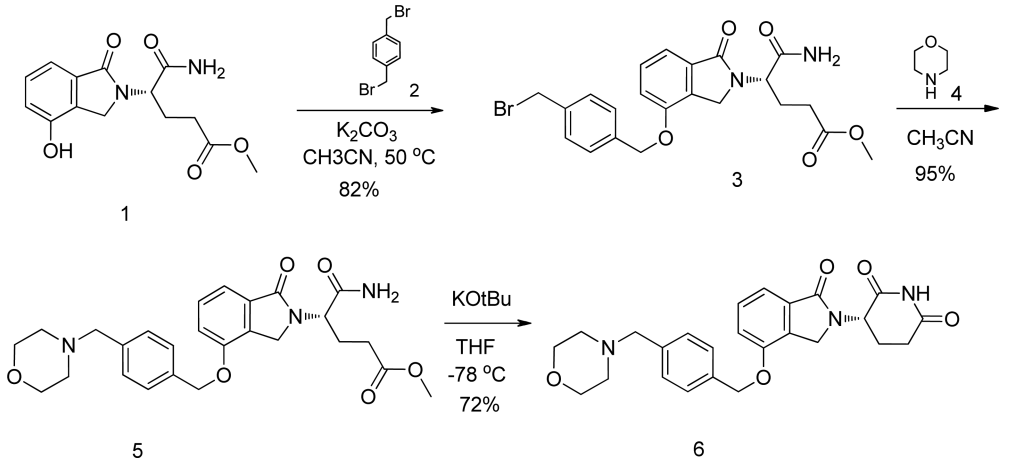


(solvent A) and 95% acetonitrile, 5% water with 0.1% phorsphoric acid (solvent B) was employed on a Waters Symmetry C18, 5 $\mu$m, 3.9 mm × 150 mm column. Flow rate was 1 mL/min, and UV detection was set to 240 nm. The LC column was maintained at ambient temperature.

**Chiral HPLC Method.** An isocratic gradient using 50% 10 mM $NH_4OAc$ in $H_2O$ (sovlent A) and 50% acetonitrile (solvent B) was employed on a CHIRALPAK AGP, 5 $\mu$m, 4.0 mm × 150 mm column. Flow rate was 1 mL/min, and UV detection was set to 240 nm. The LC column was maintained at ambient temperature.

**Synthesis of Compound 6 (Scheme 1).** As shown in Scheme 1, the synthesis started with optically pure (*S*)-3-(4-hydroxy-1-oxo-1,3-dihydroisoindol-2-yl)piperidine-2,6-dione (**1**), which was alkylated with 1,4-bis(bromomethyl)benzene (**2**) in the presence of potassium carbonate to furnish bromide (**3**). Reaction of the bromide (**3**) with morpholine (**4**) afforded **5**. Subsequent cyclization of **5** with potassium *tert*-butoxide at −78 °C proceeded to give imide (compound **6**) in a yield of 82% with a HPLC purity of 98.5%. The configuration of compound **1** was assigned based on the commercially available startling material, (*S*)-methyl 4,5-diamino-5-oxopentanoate hydrochloride. The configuration and chiral purity of **3** and **5** were not measured. However, the chiral purity of compound **6** was determined to be greater than 99% by chiral HPLC. Thus, the configuration of compound **6** was assigned as the *S*-isomer. Compound **6** is chirally stable in vivo. During DMPK study dosing with compound **6** (ee >99%), *R*-enantiomer was observed at low levels (<3% in monkey and <6% in rat).

*(S)-3-(4-Hydroxy-1-oxo-1,3-dihydroisoindol-2-yl)piperidine-2,6-dione (**1**).* (*S*)-methyl 4,5-diamino-5-oxopentanoate hydrochloride (58.7 g, 299 mmol) was added to a solution of methyl 2-(bromomethyl)-3-(*tert*-butyldimethylsilyloxy)benzoate (113 g, 299 mmol) in acetonitrile (1 L) to form a suspension. *N*-Ethyl-*N*-isopropylpropan-2-amine (104 mL, 597 mmol) was then added, and the resulting mixture was stirred at 40 °C overnight. The reaction mixture was concentrated under vacuum to give yellow solid. The solid was dissolved in ether (900 mL) and washed by aq HCl (1N, 750 mL), satd aq $NaHCO_3$ (2 × 350 mL), and brine (600 mL). The organic layer was concentrated to give (*S*)-methyl 5-amino-4-(4-(*tert*-butyldimethylsilyloxy)-1-oxoisoindolin-2-yl)-5-oxopentanoate as yellow oil. Without further purification, to the oil was added DMF (500 mL) and water (55 mL). The solution was added to $K_2CO_3$ (16.18 g, 117 mmol). The resulting suspension was stirred at room temperature for 1 h. HCl (12N, 19.5 mL) and acetonitrile (290 mL) were then added to the suspension. The resulting suspension was filtered, and the filtrate was concentrated in vacuo. Then 70 mL of acetonitrile was added to the resulting oil and heated to 50 °C until a solution formed. The solution was cooled gradually to room temperature, and the resulting suspension was filtered. Solid was dried to give compound **1** (25 g, 30%); HPLC purity 97.6%; mp 163−165 °C. $^1$H NMR (DMSO-$d_6$) $\delta$ 1.33 (s, 9 H), 1.88−2.08 (m, 1 H), 2.08−2.27 (m, 3 H), 4.32 (d, $J$ = 17.42 Hz, 1 H), 4.49 (d, $J$ = 17.42 Hz, 1 H), 4.72 (dd, $J$ = 10.22, 4.26 Hz, 1 H), 6.92−7.08 (m, 1 H), 7.09−7.26 (m, 2 H), 7.26−7.47 (m, 1 H), 7.57 (s, 1 H), 10.04 (s, 1 H). $^{13}$C NMR (DMSO-$d_6$) $\delta$ 24.86, 30.32, 44.76, 51.24, 53.30, 113.63, 117.78, 128.15, 128.20, 133.51, 152.44, 168.13, 171.76, 172.48. LCMS: M + 1 279. Anal. Calcd for $C_{14}H_{16}N_2O_5$: C, 57.53; H, 5.52; N, 9.58. Found: C, 57.35; H, 5.27; N, 9.45.

*4-[4-(4-Bromomethylbenzyloxy)-l-oxo-1,3-dihydro-isoindol-2-yl]-4-carbamoylbutyric Acid Methyl Ester (**3**).* In a 2 L round-bottom flask were charged (*S*)-methyl 5-amino-4-(4-hydroxy-l-oxoisoindolin-2-yl)-5-oxopentanoate (**1**) (30 g, 103 mmol), 1,4-bis(bromomethyl)-benzene (**2**) (81 g, 308 mmol), potassium carbonate (14.19 g, 103 mmol), and acetonitrile (1.2 L). The mixture was stirred at 50 °C for 12 h then cooled to room temperature. The mixture was filtered, and the filtrate was concentrated on rota-vap. The resulting solid was dissolved in $CH_2Cl_2$ and purified on silica gel columns eluted with $CH_2Cl_2$/MeOH to give 4-[4-(4-bromomethylbenzyloxy)-l-oxo-1,3-dihydro-isoindol-2-yl]-4-carbamoylbutyric acid methyl ester (**3**) as white solid (40 g, 82% yield). $^1$H NMR (DMSO-$d_6$) $\delta$ 1.98−2.13 (m, 1H, CHH), 2.14−2.23 (m, 1H, CHH), 2.23−2.32 (m, 2H, CHH, CHH), 3.50 (s, 3H, $CH_3$), 4.34−4.63 (m, 2H, $CH_2$), 4.67−4.80 (m, 3H, $CH_2$, NCH), 5.25 (s, 4H, $CH_2$), 7.19 (s, 1H, NHH), 7.24−7.34 (m, 2H, Ar), 7.41−7.54 (m, 5H, Ar), 7.58 (br s, 1H, NHH). LCMS: M + 1 475.

*4-Carbamoyl-4-[4-(4-morpholin-4-ylmethyl-benzyloxy)-l -oxo-1,3-dihydro-isoindol-2-yl]-butyric Acid Methyl Ester (**5**).* Morpholine (**4**) (14.72 mL, 169 mmol) was added to the $CH_2Cl_2$ solution of methyl 5-amino- 4-(4-(4-(bromomethyl)benzyloxy)-l-oxoisoindolin-2-yl)-5-oxopentanoate (**3**) (36.5 g, 77 mmol) at room temperature. The mixture was stirred at room temperature for 1 h. The resulting suspension was filtered, and the filtrate was concentrated on rota-vap. The resulting oil was dissolved in EtOAc and washed with water (50 mL × 3). The organic layer was concentrated on rota-vap to give 4-carbamoyl-4-[4-(4-morpholin-4-ylmethyl-benzyloxy)-l-oxo-1,3-dihydro-isoindol-2-yl]-butyric acid methyl ester (**5**) as a foamy solid (39 g, 95% yield); mp 66−68 °C. $^1$H NMR (DMSO-$d_6$) $\delta$ 2.00−2.12 (m, 1H, CHH), 2.14−2.22 (m, 1H, CHH), 2.22−2.29 (m, 2H, CHH, CHH), 2.30−2.39 (m, 4H, $CH_2$, $CH_2$), 3.46 (s, 2H, $CH_2$), 3.50 (s, 3H, $CH_3$), 3.53−3.63 (m, 4H, $CH_2$, $CH_2$), 4.28−4.59 (m, 2H, $CH_2$), 4.73 (dd, $J$ = 4.7, 10.2 Hz, 1H, NCH), 5.22 (s, 2H, $CH_2$), 7.14−7.23 (m, 1H, NHH), 7.26−7.39 (m, 4H, Ar), 7.41−7.51 (m, 3H, Ar), 7.58 (s, 1H, NHH). $^{13}$C NMR (DMSO-$d_6$) $\delta$ 24.82, 30.34, 44.78, 51.24, 53.12, 53.39, 62.09, 66.15, 69.35, 114.67, 115.13, 127.60, 129.00, 129.56, 130.18, 133.43, 135.32, 137.66, 153.43, 167.85, 171.74, 172.47. LCMS: M + 1 482.2. Anal. Calcd for $C_{23}H_{31}N_3O_6$ + 0.3$H_2O$: C, 64.13; H, 6.54; N, 8.63. Found: C, 63.89; H, 6.39; N, 8.56.

*3-[4-(4-Morpholin-4-ylmethyl-benzyloxy)-oxo-1,3-dihydro-isoindol-2-yl]-piperidine-2,6-dione (**6**).* To the THF solution of methyl 5-amino-4-(4-(4-(morpholinomethyl)benzyloxy)-yl-oxoisoindolin-2-yl)-5-oxopentanoate (**5**) (40 g, 83 mmol) was added potassium *tert*-butoxide (9.80 g, 87 mmol) at −78 °C. The mixture was stirred at this


DOI: 10.1021/acs.jmedchem.6b01921
J. Med. Chem. XXXX, XXX, XXX−XXX

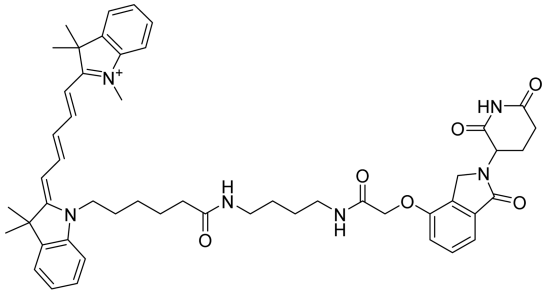

7

temperature for 30 min, then 45 mL of 1 N HCl solution was added to the reaction mixture, followed by 200 mL of saturated $NaHCO_3$ solution. The mixture was diluted with 500 mL of EtOAc at 0 °C, stirred for 5 min, and separated. The organic layer was washed with water (50 mL × 3), brine (100 mL) and concentrated on rota-vap to give a white solid, which was stirred in diethyl ether (300 mL) to give a suspension. The suspension was filtered to give 3-[4-(4-morpholin-4-ylmethyl-benzyloxy)-oxo-1,3-dihydro-isoindol-2-yl]-piperidine-2,6-dione (**6**) as white solid (28.5 g, 72% yield). HPLC: Waters Symmetry C18, 5 $\mu$m, 3.9 mm × 150 mm, 1 mL/min, 240 nm, gradient to 95/5 acetonitrile/0.1% $H_3PO_4$ in 5 min, RT = 4.78 min (98.5%); Chiral HPLC (Chiralpak AGP column, 4.0 mm × 150 mm, 5 $\mu$m particle size, isocratic 50% 10 mM $NH_4OAc$ in $H_2O$ and 50% acetonitrile) RT = 8.15 min (0.5%, *R*-isomer), RT = 10.33 min (99.5%, *S*-isomer); mp 209−211 °C. $^1$H NMR (DMSO-$d_6$) $\delta$ 1.86−2.09 (m, 1H, CHH), 2.29−2.38 (m, 4H, $CH_2$, $CH_2$), 2.44 (dd, $J$ = 4.3, 13.0 Hz, 1H, CHH), 2.53−2.64 (m, 1H, CHH), 2.82−2.99 (m, 1H, CHH), 3.46 (s, 2H, $CH_2$), 3.52−3.61 (m, 4H, $CH_2$, $CH_2$), 4.18−4.51 (m, 2H, $CH_2$), 5.11 (dd, $J$ = 5.0,13.3 Hz, 1H, NCH), 5.22 (s, 2H, $CH_2$), 7.27−7.38 (m, 5H, Ar), 7.40−7.53 (m, 3H, Ar), 10.98 (s, 1H, NH). $^{13}$C NMR (DMSO-$d_6$) $\delta$ 22.36, 31.21, 45.09, 51.58, 53.14, 62.10, 66.17, 69.41,114.97, 115.23, 127.64, 128.99, 129.81, 129.95, 133.31, 135.29, 137.68, 153.50, 168.01, 170.98, 172.83. LCMS: M + 1 465. Anal. Calcd for $C_{25}H_{27}N_3O_5$ + 0.86$H_2O$: C, 64.63; H, 6.22; N, 9.04. Found: C, 64.39; H, 6.11; N, 8.89; H2O, 3.24.

**Crystallography.** The purification of CRBN−DDB1 for crystallization was performed as previously described.[8b] Crystallization of CRBN−DDB1 with compound **6** was performed using sitting-drop vapor diffusion. Thirty mg/mL CRBN−DDB1 in the presence of 1 mM compound **6** was mixed 1:1 with, and subsequently equilibrated against, a mother liquor containing 200 mM sodium fluoride and 20% PEG 3350 at 20 C. Crystals were cryoprotected in the reservoir solution supplemented with 20% ethylene glycol and cooled under liquid nitrogen. Data was collected at the Advance Photon Source beamline LS-CAT 21ID-F. The complex crystal structure was solved by molecular replacement using Phaser with search model of 4TZ4.[9a] Subsequent manual model building using Coot and refinement were performed using Refmac5.[16] Data collection statistics and sample electron density can be found in the Supporting Information. Coordinates have been deposited in the Protein Data Bank with the accession code 5V3O.

**TR-FRET Assay.** The 6XHis-tagged full length human CRBN bound to full length human DDB1 used in the assay was purified as described elsewhere with the exception that the thrombin cleavage/ortho nickle step was removed.[8b] In the assay, 60 nM 6Xhis-tagged CRBN-DDB1 was combined with 30 nM cy5-conjugated cereblon modulator (compound 7) and 3 nM LanthaScreen Eu-anti-His Tag antibody (ThermoFisher catalogue no. PV5596) in 20 mM HEPES pH 7, 150 mM NaCl, 0.005% Tween-20 assay buffer. FRET was observed by exciting at 340 nm and monitoring emission at 615 nm (non-FRET emission) and 665 nm (FRET emission), and FRET efficiency was determined by the ratio of FRET to non-FRET emission (665 nm/615 nm). Competing cereblon modulating compound or DMSO carrier was titrated and incubated for 10 min before scanning on the Envision plate reader with a 60 $\mu$s delay to quantitate loss of FRET efficiency. All FRET competition curves were processed and evaluated using ActivityBase (IDBS), a data analysis software package.

The compound used in the FRET assay (compound 7) is: *2-((1E,3E,5Z)-5-(1-(6-((4-(2-((2-(2,6-Dioxopiperidin-3-yl)-1-oxoisoindolin-4-yl)oxy)acetamido)butyl)amino)-6-oxohexyl)-3,3-dimethylindolin-2-ylidene)penta-1,3-dien-1-yl)-1,3,3-trimethyl-3H-indol-1-ium (Compound 7).* **Cell-Based Chemiluminescent Substrate Degradation Assays.** DF15 multiple myeloma cells expressing cereblon substrates Ikaros, Aiolos, and GSPT1 fused to an ePL tag (DiscoverX) were dispensed into a 384-well plate (Corning no. 3712) prespotted with compound. Compounds were dispensed by an acoustic despenser (ATS acoustic transfer system from EDC Biosystems) into a 384-well plate in a 10-point dose response curve using 3-fold dilutions starting at 10 $\mu$M and going down to 0.0005 $\mu$M. Then 25 $\mu$L of media (RPMI-1640 + 10% heat inactivated FBS + 25 mM Hepes + 1 mM Na pyruvate + 1× NEAA + 0.1% Pluronic F-68 + 1× Pen Strep Glutamine) containing 5000 cells was dispensed per well. Assay plates were incubated at 37 °C with 5% $CO_2$ for 4 h. After incubation, 25 $\mu$L of the InCELL Hunter detection reagent working solution (DiscoverX, catalogue no. 96-0002, Fremont, CA) was added to each well and incubated at room temperature for 30 min protected from light. After 30 min, luminescence was read on a PHERAstar luminometer (Cary, NC). To determine the $EC_{50}$ value of a compound for the degradation of a given substrate (the half-maximum effective concentration), a four-parameter logistic model (sigmoidal dose−response model) (FIT = $(A + \{(B - A)/1 + [(C/x)^D]\}))$ where $C$ is the inflection point ($EC_{50}$), $D$ is the correlation coefficient, and $A$ and $B$ are the low and high limits of the fit, respectively) was used. All substrate degradation curves were processed and evaluated using ActivityBase (IDBS), a data analysis software package.

**Immunoblot Analysis of Endogenous Substrate Protein Levels.** First, 1 ×10$^6$ cells (either DF15 and OPM2) were treated with lenalidomide, pomalidomie, or compound **6** for 5 h before harvest. Then after quick 1× cold PBS rinse, cells were lysed by cell lysis buffer (Cell Signaling's Technologies). Then 10 $\mu$g of total lysate was loaded in each lane. Proteins were transferred to nitrocellulose membrane using Bio-Rad's Turbo System. Antibodies used in the Western included: Ikaros (14859S, Cell Signaling Technologies), Aiolos (15103S, Cell Signaling Technologies), actin (A5316, Sigma), and CRBN (in house antibody from Celgene).[3a]

## ■ ASSOCIATED CONTENT

### Supporting Information

The Supporting Information is available free of charge on the ACS Publications website at DOI: 10.1021/acs.jmedchem.6b01921.

Quantitation of GSPT1 degradation with chemiluminescent cell-based assay; comparison of lenalidomide and compound **6** binding modes; sample electron density from the CRBN-DDB1-compound **6** crystal structure; X-ray data and refinement statistics (PDF)

Molecular formula strings (CSV)

### Accession Codes

Coordinates for the structure of CRBN-DDB1- **6** have been deposited in the Protein Data Bank with the accession code 5V3O. Authors will release the atomic coordinates and experimental data upon article publication.

## ■ AUTHOR INFORMATION


### Corresponding Author

*Phone: 858-795-4728. E-mail: pchamberlain@celgene.com.

### ORCID

Philip P. Chamberlain: 0000-0002-6407-7344


### Notes

The authors declare the following competing financial interest(s): Authors are or have been employees, consultants, or collaborators of Celgene.



DOI: 10.1021/acs.jmedchem.6b01921
J. Med. Chem. XXXX, XXX, XXX−XXX

## ■ ACKNOWLEDGMENTS

We thank Shamrock Biostructures for data collection services. This research used resources of the Advanced Photon Source, a U.S. Department of Energy (DOE) Office of Science User Facility operated for the DOE Office of Science by Argonne National Laboratory under contract no. DE-AC02-06CH11357.

## ■ ABBREVIATIONS USED

CRBN, cereblon; IKZF1, Ikaros; IKZF3, Aiolos; SLE, systematic lupus erythematosus; MM, multiple myeloma

## ■ REFERENCES

(1) Dimopoulos, M. A.; Richardson, P. G.; Moreau, P.; Anderson, K. C. Current treatment landscape for relapsed and/or refractory multiple myeloma. *Nat. Rev. Clin. Oncol.* **2015**, *12* (1), 42−54.

(2) Ito, T.; Ando, H.; Suzuki, T.; Ogura, T.; Hotta, K.; Imamura, Y.; Yamaguchi, Y.; Handa, H. Identification of a primary target of thalidomide teratogenicity. *Science* **2010**, *327* (5971), 1345−1350.

(3) (a) Lopez-Girona, A.; Mendy, D.; Ito, T.; Miller, K.; Gandhi, A. K.; Kang, J.; Karasawa, S.; Carmel, G.; Jackson, P.; Abbasian, M.; Mahmoudi, A.; Cathers, B.; Rychak, E.; Gaidarova, S.; Chen, R.; Schafer, P. H.; Handa, H.; Daniel, T. O.; Evans, J. F.; Chopra, R. Cereblon is a direct protein target for immunomodulatory and antiproliferative activities of lenalidomide and pomalidomide. *Leukemia* **2012**, *26* (11), 2326−2335. (b) Zhu, Y. X.; Braggio, E.; Shi, C. X.; Bruins, L. A.; Schmidt, J. E.; Van Wier, S.; Chang, X. B.; Bjorklund, C. C.; Fonseca, R.; Bergsagel, P. L.; Orlowski, R. Z.; Stewart, A. K. Cereblon expression is required for the antimyeloma activity of lenalidomide and pomalidomide. *Blood* **2011**, *118* (18), 4771−4779.

(4) (a) Kronke, J.; Udeshi, N. D.; Narla, A.; Grauman, P.; Hurst, S. N.; McConkey, M.; Svinkina, T.; Heckl, D.; Comer, E.; Li, X.; Ciarlo, C.; Hartman, E.; Munshi, N.; Schenone, M.; Schreiber, S. L.; Carr, S. A.; Ebert, B. L. Lenalidomide causes selective degradation of IKZF1 and IKZF3 in multiple myeloma cells. *Science* **2014**, *343* (6168), 301−305. (b) Lu, G.; Middleton, R. E.; Sun, H.; Naniong, M.; Ott, C. J.; Mitsiades, C. S.; Wong, K. K.; Bradner, J. E.; Kaelin, W. G., Jr. The myeloma drug lenalidomide promotes the cereblon-dependent destruction of Ikaros proteins. *Science* **2014**, *343* (6168), 305−309. (c) Gandhi, A. K.; Kang, J.; Havens, C. G.; Conklin, T.; Ning, Y.; Wu, L.; Ito, T.; Ando, H.; Waldman, M. F.; Thakurta, A.; Klippel, A.; Handa, H.; Daniel, T. O.; Schafer, P. H.; Chopra, R. Immunomodulatory agents lenalidomide and pomalidomide co-stimulate T cells by inducing degradation of T cell repressors Ikaros and Aiolos via modulation of the E3 ubiquitin ligase complex CRL4(CRBN.). *Br. J. Haematol.* **2014**, *164* (6), 811−821.

(5) (a) Dijon, M.; Bardin, F.; Murati, A.; Batoz, M.; Chabannon, C.; Tonnelle, C. The role of Ikaros in human erythroid differentiation. *Blood* **2008**, *111* (3), 1138−1146. (b) John, L. B.; Ward, A. C. The Ikaros gene family: transcriptional regulators of hematopoiesis and immunity. *Mol. Immunol.* **2011**, *48* (9−10), 1272−1278.

(6) Bjorklund, C. C.; Lu, L.; Kang, J.; Hagner, P. R.; Havens, C. G.; Amatangelo, M.; Wang, M.; Ren, Y.; Couto, S.; Breider, M.; Ning, Y.; Gandhi, A. K.; Daniel, T. O.; Chopra, R.; Klippel, A.; Thakurta, A. G. Rate of CRL4(CRBN) substrate Ikaros and Aiolos degradation underlies differential activity of lenalidomide and pomalidomide in multiple myeloma cells by regulation of c-Myc and IRF4. *Blood Cancer Journal* **2015**, *5*, e354.

(7) (a) Cai, X.; Qiao, Y.; Diao, C.; Xu, X.; Chen, Y.; Du, S.; Liu, X.; Liu, N.; Yu, S.; Chen, D.; Jiang, Y. Association between polymorphisms of the IKZF3 gene and systemic lupus erythematosus in a Chinese Han population. *PLoS One* **2014**, *9* (10), e108661. (b) Cunninghame Graham, D. S.; Morris, D. L.; Bhangale, T. R.; Criswell, L. A.; Syvanen, A. C.; Ronnblom, L.; Behrens, T. W.; Graham, R. R.; Vyse, T. J. Association of NCF2, IKZF1, IRF8, IFIH1, and TYK2 with systemic lupus erythematosus. *PLoS Genet.* **2011**, *7* (10), e1002341. (c) Han, J. W.; Zheng, H. F.; Cui, Y.; Sun, L. D.; Ye, D. Q.; Hu, Z.; Xu, J. H.; Cai, Z. M.; Huang, W.; Zhao, G. P.; Xie, H. F.; Fang, H.; Lu, Q. J.; Xu, J. H.; Li, X. P.; Pan, Y. F.; Deng, D. Q.; Zeng, F. Q.; Ye, Z. Z.; Zhang, X. Y.; Wang, Q. W.; Hao, F.; Ma, L.; Zuo, X. B.; Zhou, F. S.; Du, W. H.; Cheng, Y. L.; Yang, J. Q.; Shen, S. K.; Li, J.; Sheng, Y. J.; Zuo, X. X.; Zhu, W. F.; Gao, F.; Zhang, P. L.; Guo, Q.; Li, B.; Gao, M.; Xiao, F. L.; Quan, C.; Zhang, C.; Zhang, Z.; Zhu, K. J.; Li, Y.; Hu, D. Y.; Lu, W. S.; Huang, J. L.; Liu, S. X.; Li, H.; Ren, Y. Q.; Wang, Z. X.; Yang, C. J.; Wang, P. G.; Zhou, W. M.; Lv, Y. M.; Zhang, A. P.; Zhang, S. Q.; Lin, D.; Li, Y.; Low, H. Q.; Shen, M.; Zhai, Z. F.; Wang, Y.; Zhang, F. Y.; Yang, S.; Liu, J. J.; Zhang, X. J. Genome-wide association study in a Chinese Han population identifies nine new susceptibility loci for systemic lupus erythematosus. *Nat. Genet.* **2009**, *41* (11), 1234−1237. (d) He, C. F.; Liu, Y. S.; Cheng, Y. L.; Gao, J. P.; Pan, T. M.; Han, J. W.; Quan, C.; Sun, L. D.; Zheng, H. F.; Zuo, X. B.; Xu, S. X.; Sheng, Y. J.; Yao, S.; Hu, W. L.; Li, Y.; Yu, Z. Y.; Yin, X. Y.; Zhang, X. J.; Cui, Y.; Yang, S. TNIP1, SLC15A4, ETS1, RasGRP3 and IKZF1 are associated with clinical features of systemic lupus erythematosus in a Chinese Han population. *Lupus* **2010**, *19* (10), 1181−1186. (e) Lessard, C. J.; Adrianto, I.; Ice, J. A.; Wiley, G. B.; Kelly, J. A.; Glenn, S. B.; Adler, A. J.; Li, H.; Rasmussen, A.; Williams, A. H.; Ziegler, J.; Comeau, M. E.; Marion, M.; Wakeland, B. E.; Liang, C.; Ramos, P. S.; Grundahl, K. M.; Gallant, C. J.; Alarcon-Riquelme, M. E.; Alarcon, G. S.; Anaya, J. M.; Bae, S. C.; Boackle, S. A.; Brown, E. E.; Chang, D. M.; Cho, S. K.; Criswell, L. A.; Edberg, J. C.; Freedman, B. I.; Gilkeson, G. S.; Jacob, C. O.; James, J. A.; Kamen, D. L.; Kimberly, R. P.; Kim, J. H.; Martin, J.; Merrill, J. T.; Niewold, T. B.; Park, S. Y.; Petri, M. A.; Pons-Estel, B. A.; Ramsey-Goldman, R.; Reveille, J. D.; Scofield, R. H.; Song, Y. W.; Stevens, A. M.; Tsao, B. P.; Vila, L. M.; Vyse, T. J.; Yu, C. Y.; Guthridge, J. M.; Kaufman, K. M.; Harley, J. B.; Wakeland, E. K.; Langefeld, C. D.; Gaffney, P. M.; Montgomery, C. G.; Moser, K. L. Identification of IRF8, TMEM39A, and IKZF3-ZPBP2 as susceptibility loci for systemic lupus erythematosus in a large-scale multiracial replication study. *Am. J. Hum. Genet.* **2012**, *90* (4), 648−660.

(8) (a) Kronke, J.; Fink, E. C.; Hollenbach, P. W.; MacBeth, K. J.; Hurst, S. N.; Udeshi, N. D.; Chamberlain, P. P.; Mani, D. R.; Man, H. W.; Gandhi, A. K.; Svinkina, T.; Schneider, R. K.; McConkey, M.; Jaras, M.; Griffiths, E.; Wetzler, M.; Bullinger, L.; Cathers, B. E.; Carr, S. A.; Chopra, R.; Ebert, B. L. Lenalidomide induces ubiquitination and degradation of CK1alpha in del(5q) MDS. *Nature* **2015**, *523* (7559), 183−188. (b) Matyskiela, M. E.; Lu, G.; Ito, T.; Pagarigan, B.; Lu, C. C.; Miller, K.; Fang, W.; Wang, N. Y.; Nguyen, D.; Houston, J.; Carmel, G.; Tran, T.; Riley, M.; Nosaka, L.; Lander, G. C.; Gaidarova, S.; Xu, S.; Ruchelman, A. L.; Handa, H.; Carmichael, J.; Daniel, T. O.; Cathers, B. E.; Lopez-Girona, A.; Chamberlain, P. P. A novel cereblon modulator recruits GSPT1 to the CRL4(CRBN) ubiquitin ligase. *Nature* **2016**, *535* (7611), 252−257.

(9) (a) Chamberlain, P. P.; Lopez-Girona, A.; Miller, K.; Carmel, G.; Pagarigan, B.; Chie-Leon, B.; Rychak, E.; Corral, L. G.; Ren, Y. J.; Wang, M.; Riley, M.; Delker, S. L.; Ito, T.; Ando, H.; Mori, T.; Hirano, Y.; Handa, H.; Hakoshima, T.; Daniel, T. O.; Cathers, B. E. Structure of the human Cereblon-DDB1-lenalidomide complex reveals basis for responsiveness to thalidomide analogs. *Nat. Struct. Mol. Biol.* **2014**, *21* (9), 803−809. (b) Fischer, E. S.; Bohm, K.; Lydeard, J. R.; Yang, H.; Stadler, M. B.; Cavadini, S.; Nagel, J.; Serluca, F.; Acker, V.; Lingaraju, G. M.; Tichkule, R. B.; Schebesta, M.; Forrester, W. C.; Schirle, M.; Hassiepen, U.; Ottl, J.; Hild, M.; Beckwith, R. E.; Harper, J. W.; Jenkins, J. L.; Thoma, N. H. Structure of the DDB1-CRBN E3 ubiquitin ligase in complex with thalidomide. *Nature* **2014**, *512* (7512), 49−53.

(10) Petzold, G.; Fischer, E. S.; Thoma, N. H. Structural basis of lenalidomide-induced CK1alpha degradation by the CRL4(CRBN) ubiquitin ligase. *Nature* **2016**, *532* (7597), 127−130.

(11) (a) Sheard, L. B.; Tan, X.; Mao, H.; Withers, J.; Ben-Nissan, G.; Hinds, T. R.; Kobayashi, Y.; Hsu, F. F.; Sharon, M.; Browse, J.; He, S. Y.; Rizo, J.; Howe, G. A.; Zheng, N. Jasmonate perception by inositol-phosphate-potentiated COI1-JAZ co-receptor. *Nature* **2010**, *468* (7322), 400−405. (b) Tan, X.; Calderon-Villalobos, L. I.; Sharon, M.; Zheng, C.; Robinson, C. V.; Estelle, M.; Zheng, N. Mechanism of



DOI: 10.1021/acs.jmedchem.6b01921
J. Med. Chem. XXXX, XXX, XXX−XXX

auxin perception by the TIR1 ubiquitin ligase. *Nature* **2007**, *446* (7136), 640−645.
(12) (a) Deshaies, R. J. Protein degradation: Prime time for PROTACs. *Nat. Chem. Biol.* **2015**, *11* (9), 634−635. (b) Toure, M.; Crews, C. M. Small-molecule PROTACS: new approaches to protein degradation. *Angew. Chem., Int. Ed.* **2016**, *55* (6), 1966−1973.
(13) Man, H.; Muller, G. W.; Ruchelman, A. L.; Khalil, E. M.; Chen, R. S.; Zhang, W., Arylmethoxy isoindolinone derivatives and compositions comprising and methods of using the same. US Patent 8,518,972, 2013.
(14) Boichenko, I.; Deiss, S.; Bar, K.; Hartmann, M. D.; Hernandez Alvarez, B. A FRET-based assay for the identification and characterization of cereblon ligands. *J. Med. Chem.* **2016**, *59* (2), 770−774.
(15) Katagiri, S.; Yonezawa, T.; Kuyama, J.; Kanayama, Y.; Tamaki, T.; Ohnishi, M.; Tarui, S.; Nishida, K.; Abe, T. Two distinct human myeloma cell lines originating from one patient with myeloma. *Int. J. Cancer* **1985**, *36* (2), 241−246.
(16) (a) Emsley, P.; Lohkamp, B.; Scott, W. G.; Cowtan, K. Features and development of Coot. *Acta Crystallogr., Sect. D: Biol. Crystallogr.* **2010**, *66* (4), 486−501. (b) Murshudov, G. N.; Skubak, P.; Lebedev, A. A.; Pannu, N. S.; Steiner, R. A.; Nicholls, R. A.; Winn, M. D.; Long, F.; Vagin, A. A. REFMAC5 for the refinement of macromolecular crystal structures. *Acta Crystallogr., Sect. D: Biol. Crystallogr.* **2011**, *67* (4), 355−367.



DOI: 10.1021/acs.jmedchem.6b01921
*J. Med. Chem.* XXXX, XXX, XXX−XXX